



Cite this: DOI: 10.1039/d0cc06840c

 Received 13th October 2020,
Accepted 18th November 2020

DOI: 10.1039/d0cc06840c

rsc.li/chemcomm

Tunable iridium catalyst designs with bidentate N-heterocyclic carbene ligands for SABRE hyperpolarization of sterically hindered substrates†

 Pierce Pham  and Christian Hilty *

A series of bidentate N-heterocyclic carbene (NHC) iridium catalysts, [Ir(κ C,N-NHC)H₂L₂]BPh₄, are proposed for SABRE hyperpolarization. The steric and electronic properties of the NHCs are used to tune substrate affinity and thereby SABRE efficiency. The sterically hindered substrates 2,4-diaminopyrimidine and trimethoprim yielded maximum proton NMR signal enhancements of ~300-fold and ~150-fold, respectively.

The signal amplification by reversible exchange (SABRE)^{1,2} provides renewable nuclear spin hyperpolarization, which can potentially further a wide array of applications of NMR. Particularly, biomedical and biomolecular applications often are limited by achievable sensitivity at a low analyte concentration. SABRE hyperpolarization would allow the measurement of multi-dimensional spectra for structure elucidations, as well as of time-resolved data showing the evolution of biochemical processes and reactions.

Para-Hydrogen and *ortho*-hydrogen are the singlet and triplet spin states of hydrogen molecules. The *para* state can be enriched at low temperature using a spin flip catalyst. In the SABRE process, a net nuclear spin polarization of a target compound is achieved when the target compound and *para*-hydrogen simultaneously bind to a polarization transfer catalyst, such as an iridium complex. A primary challenge in the applications of SABRE at present is the need for broadening the range of compounds that can be hyperpolarized with this technique. In order to build bulk spin polarization, the analyte must be a ligand to the SABRE catalyst with specific properties. Only substrates that bind with optimal affinity to the metal center of the catalyst while forming a structure with a nuclear spin J-coupling to metal hydrides, originating from *para*-hydrogen, can

receive spin polarization.^{1–3} In general, many nitrogen-heterocyclic compounds may fulfil these requirements and the typical pre-catalyst, Ir(COD)(Cl)(IMes), is commonly employed for SABRE (IMes = 1,3-bis(2,4,6-trimethylphenyl)imidazol-2-ylidene) and (COD = 1,5-cyclooctadiene). The prototypical ligand pyridine readily achieves proton NMR signal enhancements of several hundred-fold. However, modifications of the ligand structure, such as substitutions with different functional groups, can modify binding affinity or exchange rates, decisively lowering the achievable hyperpolarization.^{4,5} These issues can be overcome for different substrates by changing the catalyst structure, such as by modifying the IMes ligand or including co-ligands binding to the catalyst.^{6–11}

Using monodentate NHC, three bound substrate molecules are required to form SABRE active complexes. This requirement prevents hyperpolarization of molecules with bulky functional groups near their binding site.^{2–7} This steric hindrance can be alleviated with the replacement of at least one bound substrate molecule by a co-ligand such as acetonitrile or allylamine. A proton signal enhancement of up to several hundred-fold has been achieved for *ortho*-substituted pyridines and pyrimidines with this strategy.¹² Similarly, iridium catalysts with bidentate ligands can form SABRE active complexes with two bound substrates, solving the steric congestion of ligand binding. SABRE hyperpolarization of 2-methylpyridine and 2-fluoropyridine to proton signal enhancements of >100-fold was demonstrated using [Ir(COD)(Phox)]PF₆ (Phox = 2-(2-(diphenylphosphanyl)phenyl)-4,5-dihydrooxazole). This catalyst was originally used as a hydrogenation catalyst.¹³ Several iridium complexes with bidentate NHC ligands are also known to catalyze hydrogenation and dehydrogenation reactions,^{14–17} and are potentially suitable for SABRE.

Here, we demonstrate the hyperpolarization of sterically hindered compounds using iridium catalysts with a series of bidentate NHC ligands that have different steric and electronic properties. These NHC ligands structurally include aryl groups and nitrogen-heterocyclic groups. The aryl groups include 2,4,6-trimethylphenyl, resembling a typical IMes-iridium

Chemistry Department, Texas A&M University, 3255 TAMU, College Station, TX 77843, USA. E-mail: chilty@tamu.edu

† Electronic supplementary information (ESI) available: Analytical methods, synthesis and characterization, parahydrogen generation, pre-catalyst activation and SABRE experiments, dissociation rates of bound ligands, and determination of T₁ relaxation values. CCDC 2016119. For ESI and crystallographic data in CIF or other electronic format see DOI: 10.1039/d0cc06840c

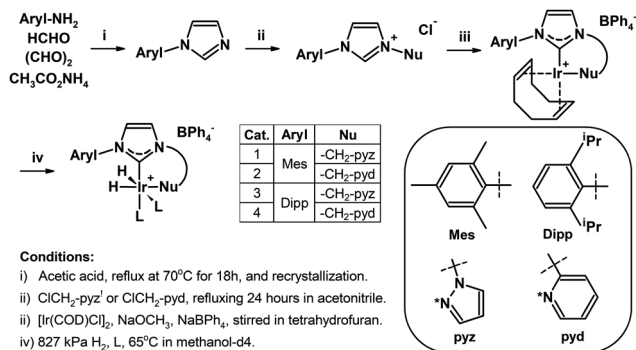


Fig. 1 Synthetic scheme for the four catalysts (steps i–iii, see ESI†), and activation (step iv) of [Ir(COD)(κC,N-NHC)]BPh₄ for hyperpolarization of a substrate L. Catalyst structures are shown described in the table and inset. Ph = phenyl, Mes = 2,4,6-trimethylphenyl, Dipp = 2,6-diisopropylphenyl, pyz = 1-pyrazolyl, pyd = 2-pyridyl, and COD = (Z,Z)-1,5-cyclooctadiene. ! *In situ* product of thionyl chloride and 1-pyrazolylmethanol. * Binding sites of the bidentate NHC ligands to iridium.

SABRE catalyst, and 2,6-diisopropylphenyl that causes higher steric hindrance. The selected nitrogen-heterocyclic groups mimic hyperpolarizable substrates including pyrazole and pyridine, with the pyridyl fragment showing higher electron donation to the Ir center (Fig. 1).

After activation of pre-catalysts, SABRE experiments were conducted by bubbling 10-bar hydrogen gas (~50% *para*-hydrogen) through the samples for 15 seconds at pre-set temperature and magnetic field, followed by the manual transfer of the samples into an NMR magnet within 5 seconds. The proton NMR spectra were collected after a 90° hard pulse (see ESI†).

For the substrate 2,4-diaminopyrimidine and all four catalysts, SABRE hyperpolarization with a proton NMR signal enhancement of several hundred-fold was obtained, as compared to signal integrals from thermal polarization in a 400 MHz NMR magnet (Fig. 2a–d for catalysts 1–4). The *ortho*-proton (7.67 ppm in Fig. 2a–d) to N1, the likely binding site of 2,4-diaminopyrimidine, as expected

received the highest polarization. The spin polarization achieved for this substrate was higher than with a typical IMes-iridium catalyst both with and without coligands, which had previously resulted in signal enhancements of 7 and 210 fold, respectively.¹² In Fig. 2e, the larger drug molecule trimethoprim, which contains the same fragment, is hyperpolarized with the catalyst 4. Again, the *ortho*-proton (7.53 ppm in Fig. 2e) to N1 of pyrimidinyl moiety, shows a signal enhancement of >100-fold, demonstrating that the bidentate catalyst is capable of binding to, and therefore enable the hyperpolarization of larger molecules. The signal enhancement of 148-fold is approximately two times higher than an enhancement of 70-fold achieved with IMes-iridium catalyst with coligands under optimal conditions.¹²

The SABRE polarization efficiency with the different catalysts depends on several factors, which include catalyst and substrate concentrations, *para*-hydrogen enrichment and pressure, magnetic field, and temperature. The magnetic field and temperature dependence for SABRE hyperpolarization of 2,4-diaminopyrimidine using catalysts 1–4 is characterized in Fig. 3a and b, respectively. The signal enhancements of the proton *ortho* to the likely binding site of the substrate are plotted. First, magnetic fields were tested in the range of 1–10 mT, while keeping the sample at a constant temperature of 35 °C during polarization (Fig. 3a). Although different signal enhancements were obtained using the different catalysts, a similar trend is observed. As magnetic fields increase, enhancements generally increase up to a field of 6–7 mT and decreased thereafter. This optimal field is in agreement with predictions of ~6 mT for other Ir catalysts based on level crossing theory.¹⁸ The magnetic field was chosen at 6.5 mT, which is also a typical field strength for pyridine hyperpolarization with Ir catalysts.^{3,9,19}

In contrast, at a constant magnetic field, a difference in the temperature dependence of the signal enhancements with the four catalysts was observed. The signals obtained using catalysts 1 and 2 increased monotonically as the temperature was

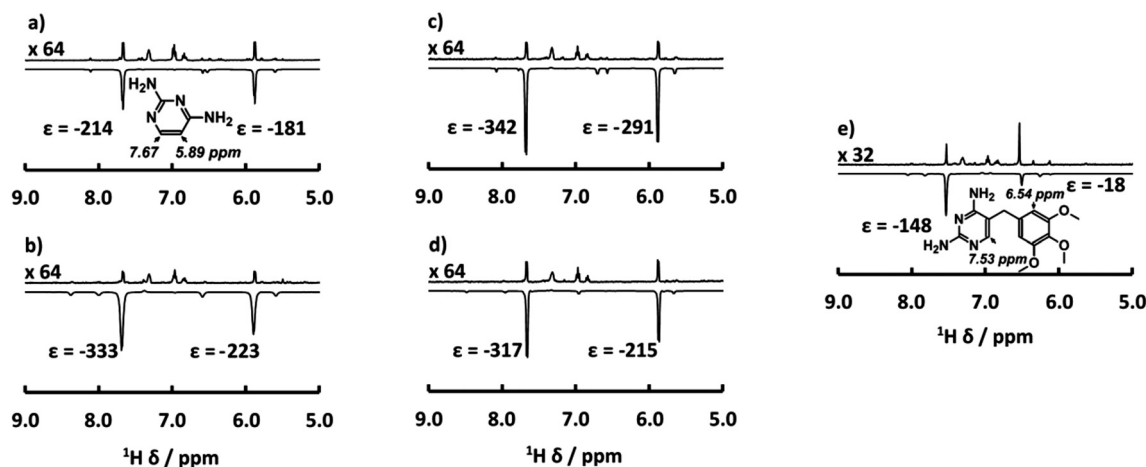


Fig. 2 Proton NMR spectra of 2,4-diaminopyrimidine hyperpolarized using catalysts 1–4 in (a–d), respectively, and trimethoprim hyperpolarized using catalyst 4 in (e). Each panel contains the SABRE hyperpolarized spectrum obtained under optimal conditions shown in Table 1 (bottom trace) and a non-hyperpolarized reference spectrum obtained at 25 °C (top trace).

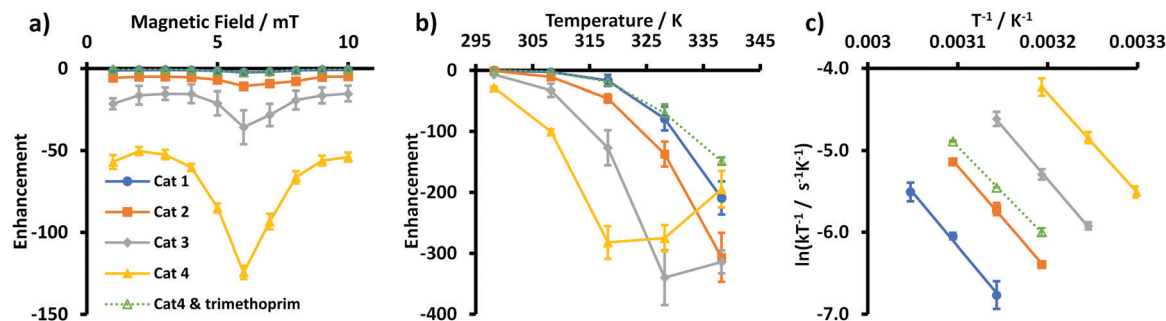


Fig. 3 (a) Magnetic field dependence of signal enhancement from SABRE hyperpolarization of the *ortho*-proton in 2,4-diaminopyrimidine using catalysts 1–4 and the *ortho*-proton of trimethoprim using catalyst 4. The temperature for hyperpolarization was 35 °C. (b) Temperature dependence of signal enhancement. The data was measured at a magnetic field of 6.5 mT. (c) Eyring plots showing the temperature dependence of the ligand exchange rates determined from exchange spectroscopy (EXSY). The lines represent the linear fitting results of $y = -13147x + 35$ ($R^2 = 0.99$), $y = -12694x + 34$ ($R^2 = 1.00$), $y = -12847x + 36$ ($R^2 = 1.00$), and $y = -11231x + 35$ ($R^2 = 1.00$) for the experiments of 2,4-diaminopyrimidine and catalysts 1–4 respectively and $-11231x + 30$ ($R^2 = 1.00$) for the experiment of trimethoprim with catalyst 4.

increased up to 65 °C. Substrates hyperpolarized with catalysts 3 and 4 on the other hand reached a maximum signal enhancement near 55 and 45 °C, respectively. The different temperatures for maximum signal enhancement can be rationalized by analyzing the dissociation rates of the bound substrates from the catalyst. Several systematic studies previously indicated that the SABRE signal enhancement depends strongly on ligand exchange rates, with rates that are too high or too low resulting in lower signals.^{3,19} For the catalysts described here, the 2,6-diisopropylphenyl group causes more steric hindrance than the 2,4,6-trimethylphenyl group, thereby increasing the substrate dissociation rate. The pyridyl moiety, based on the basicity of comparable monodentate ligands, is expected to be a stronger electron donor compared to the pyrazolyl moiety,²¹ and therefore caused an increased substrate dissociation rate. Overall, catalyst 4, which contains the moieties with higher steric hindrance and higher electron donation reached the optimal ligand exchange rate at the lowest temperature.

Optimal substrate exchange rates in the range of 10–12 s⁻¹ were previously described for equatorially bound ligands in hyperpolarization of pyridine using the typical Ir(IMes)(pyridine)₃H₂ catalyst.^{2,3} For comparison, we determined the dissociation rates of equatorially bound 2,4-diaminopyrimidine from catalysts 1–4 in experiments separate from those showing hyperpolarized signals. The corresponding Eyring plots are shown in Fig. 3c. The assumption that the optimal exchange rate for

SABRE polarization is on the order of 10 s⁻¹ would predict optimal temperatures of 71.7, 63.8, 54.2, and 46.2 °C for catalysts 1–4, respectively. These values were determined from the fitting results in Fig. 3c. The predicted temperatures for optimal SABRE signal enhancements agree with the observed temperatures of 55 and 45 °C for catalysts 3 and 4, for which the optimal temperatures were within the experimentally accessible range.

The conditions for highest signal enhancement are summarized in Table 1. As seen in the individual spectra from Fig. 2, signal enhancements of the proton in the *ortho* position to the catalyst binding site of 2,4-diaminopyrimidine were achieved at ~200-fold for catalyst 1 and ~300-fold for catalysts 2–4. Based on the observed trends, it is likely that an enhancement of similar magnitude may also be achieved for catalyst 1, if a higher temperature would be reached.

The data in Fig. 3c and Table 1 demonstrates that the exchange rate can be tuned both by changing the steric and electronic properties of the bidentate catalysts, to achieve an optimum polarization at a desired temperature. For 2,4-diaminopyrimidine, the steric hindrance of the bidentate NHC ligands influenced the exchange rates of 2,4-diaminopyrimidine more strongly than the electronic properties, as evidenced by comparing ligand dissociation rates of catalyst 1 to catalyst 2 (stronger electron donation) or catalyst 3 (higher steric hindrance) (Fig. 3c).

Table 1 Summary of activation, optimization, and enhancements for SABRE hyperpolarization of 2,4-diaminopyrimidine using catalysts 1–4, and for trimethoprim with catalyst 4

Catalyst	1	2	3	4	4 + trimethoprim
Activation conditions ^a	827 kPa H ₂ , 65 °C 2 hours	10 minutes	20 minutes	10 minutes	10 minutes
SABRE conditions	827 kPa H ₂ 65 °C	65 °C	55 °C	45 °C	65 °C
Signal enhancements ^b	-209 ± 27 -160 ± 23	-307 ± 40 -217 ± 19	-340 ± 45 -302 ± 32	-282 ± 27 -204 ± 8	-149 ± 6 ^c -16 ± 2 ^c

^a The first NMR scan was obtained 10 minutes after pressurization with hydrogen gas. ^b Signal enhancements of *ortho*-proton (top) and *meta*-proton (bottom) of 2,4-diaminopyrimidine. ^c Enhancements of pyrimidinyl proton (top) and phenyl proton (bottom) of trimethoprim. The standard deviations are calculated from a total of four measurements made from two distinct samples.

In the following, hyperpolarization of the substrate trimethoprim using catalyst 4 is analyzed. Because of the larger size, trimethoprim may be expected to reach the optimal SABRE condition at lower temperature than 2,4-diaminopyrimidine. However, the highest signal enhancement was observed at 65 °C, in agreement with a temperature of 63.4 °C predicted from the Eyring plot in Fig. 3c for a dissociation rate of 10 s⁻¹. This temperature is higher than the optimal temperature of 45 °C for hyperpolarizing 2,4-diaminopyrimidine with the same catalyst. This observation can be rationalized by the benzyl-type substituent of trimethoprim causing an increase in the electron donating ability of N1 in the pyrimidine fragment, and thereby a stronger binding of trimethoprim to iridium. As also seen in Fig. 2, a proton NMR signal enhancement of near 150 was achieved, about twice as much as with a monodentate catalyst,¹² but lower than for 2,4-diaminopyrimidine. This latter difference is likely due to the different *T*₁ relaxation time⁵ of trimethoprim and 2,4-diaminopyrimidine, which are 2.3 and 10.3 s, respectively, at 9.4 T.

There is not a single catalyst to provide high SABRE efficiency to all ligands. After the first SABRE demonstration with pyridine using Crabtree's catalyst, multiple iridium catalysts with different monodentate phosphine ligands were investigated. The usage of monodentate NHC iridium catalysts showed faster exchange rates and higher SABRE activity for pyridine.^{2,20} An iridium catalyst with bidentate phosphine ligand demonstrated good SABRE activities for hyperpolarization 2-methylpyridine and 2-fluoropyridine.¹³ The phosphine ligand may not yield similar SABRE activities for ligands with stronger binding affinity such as 2,4-diaminopyrimidine due to slow ligand exchange rates.

Here, we describe a series of bidentate based on an NHC core structure, which can be tuned for substrate binding affinity by variation of steric and electron donating properties. The bidentate ligand structure is well suited for this goal, by offering two separate sites for these modifications. Additional variations can readily be envisaged to support hyperpolarization of more strongly binding substrates, by replacing the aryl moiety with analogs of 2,6-diisopropylphenyl that contain longer chains or bulkier substituents, and the nucleophilic moiety with stronger electron donating groups such as carbenes.^{22,23} Additional increases in signal enhancement could further be achieved without any modification of the catalyst, by using higher *para*-hydrogen enrichment at lower temperature, or catalysts with deuterated NHC ligand.¹⁹ The same catalysts may also be amenable to hyperpolarize heteronuclei such as ¹⁵N or ¹³C, either directly or indirectly.^{7,13}

In conclusion, a series of four bidentate-NHC iridium catalysts rationalize the influence of steric and electronic effects to the SABRE hyperpolarization of substrates containing N-heterocycles. The SABRE enhancements of the *ortho*-proton to N1 reached ~300-fold for the *ortho*-substituted heterocycle 2,4-diaminopyrimidine, and ~150-fold for trimethoprim, a bulkier molecule containing this fragment. A comparison of substrate exchange rates and optimal conditions for hyperpolarization emphasizes the importance of the catalyst design for strongly binding ligands. Broadening the range of catalyst designs

available for SABRE hyperpolarization is crucial to enhance the application of this technique, especially towards large libraries of biological compounds encountered in drug discovery and other applications.

Financial support from the National Science Foundation (Grant CHE-1900406) and from the Welch Foundation (Grant A-1658) is gratefully acknowledged. We thank Trung Huu Le for assistance with X-ray crystallography.

Conflicts of interest

There are no conflicts to declare.

Notes and references

- 1 R. W. Adams, J. A. Aguilar, K. D. Atkinson, M. J. Cowley, P. I. P. Elliott, S. B. Duckett, G. G. R. Green, I. G. Khazal, J. López-Serrano and D. C. Williamson, *Science*, 2009, **323**, 1708–1711.
- 2 M. J. Cowley, R. W. Adams, K. D. Atkinson, M. C. R. Cockett, S. B. Duckett, G. G. R. Green, J. A. B. Lohman, R. Kerssebaum, D. Kilgour and R. E. Mewis, *J. Am. Chem. Soc.*, 2011, **133**, 6134–6137.
- 3 B. J. A. van Weerdenburg, S. Glöggl, N. Eshuis, A. H. J. (Ton) Engwerda, J. M. M. Smits, R. de Gelder, S. Appelt, S. S. Wymenga, M. Tessari, M. C. Feiters, B. Blümich and F. P. J. T. Rutjes, *Chem. Commun.*, 2013, **49**, 7388–7390.
- 4 R. V. Shchepin, M. L. Truong, T. Theis, A. M. Coffey, F. Shi, K. W. Waddell, W. S. Warren, B. M. Goodson and E. Y. Chekmenev, *J. Phys. Chem. Lett.*, 2015, **6**, 1961–1967.
- 5 E. V. Stanbury, P. M. Richardson and S. B. Duckett, *Catal. Sci. Technol.*, 2019, **9**, 3914–3922.
- 6 W. Iali, P. J. Rayner, A. Alshehri, A. J. Holmes, A. J. Ruddlesden and S. B. Duckett, *Chem. Sci.*, 2018, **9**, 3677–3684.
- 7 W. Iali, P. J. Rayner and S. B. Duckett, *Sci. Adv.*, 2018, **4**, eaao6250.
- 8 C. M. Wong, M. Fekete, R. Nelson-Forde, M. R. D. Gatus, P. J. Rayner, A. C. Whitwood, S. B. Duckett and B. A. Messerle, *Catal. Sci. Technol.*, 2018, **8**, 4925–4933.
- 9 A. J. Ruddlesden and S. B. Duckett, *Chem. Commun.*, 2016, **52**, 8467–8470.
- 10 F. Shi, P. He, Q. A. Best, K. Groome, M. L. Truong, A. M. Coffey, G. Zimay, R. V. Shchepin, K. W. Waddell, E. Y. Chekmenev and B. M. Goodson, *J. Phys. Chem. C*, 2016, **120**, 12149–12156.
- 11 M. Fekete, C. Gibard, G. J. Dear, G. G. R. Green, A. J. J. Hooper, A. D. Roberts, F. Cisnetti and S. B. Duckett, *Dalton Trans.*, 2015, **44**, 7870–7880.
- 12 R. Mandal, P. Pham and C. Hilty, *ChemPhysChem*, 2020, **21**, 2166–2172.
- 13 J. F. P. Colell, A. W. J. Logan, Z. Zhou, J. R. Lindale, R. Laasner, R. V. Shchepin, E. Y. Chekmenev, V. Blum, W. S. Warren, S. J. Malcolmson and T. Theis, *Chem. Commun.*, 2020, **56**, 9336–9339.
- 14 S. Gruber, M. Neuburger and A. Pfaltz, *Organometallics*, 2013, **32**, 4702–4711.
- 15 C. Diez and U. Nagel, *Appl. Organomet. Chem.*, 2010, **24**, 509–516.
- 16 A. Schumacher, M. Bernasconi and A. Pfaltz, *Angew. Chem., Int. Ed.*, 2013, **52**, 7422–7425.
- 17 K. Y. Wan, F. Roelfes, A. J. Lough, F. E. Hahn and R. H. Morris, *Organometallics*, 2018, **37**, 491–504.
- 18 A. N. Pravidtsev, K. L. Ivanov, A. V. Yurkovskaya, P. A. Petrov, H.-H. Limbach, R. Kaptein and H.-M. Vieth, *J. Magn. Reson.*, 2015, **261**, 73–82.
- 19 P. J. Rayner, P. Norcott, K. M. Appleby, W. Iali, R. O. John, S. J. Hart, A. C. Whitwood and S. B. Duckett, *Nat. Commun.*, 2018, **9**, 1–11.
- 20 K. D. Atkinson, M. J. Cowley, P. I. P. Elliott, S. B. Duckett, G. G. R. Green, J. López-Serrano and A. C. Whitwood, *J. Am. Chem. Soc.*, 2009, **131**, 13362–13368.
- 21 1-methylpyrazole conjugate has p*K*_a of 2.09. T. Asami, T. Matsuo, T. Fukuyama, Y. Ie, F. Kakiuchi and N. Chatani, *J. Org. Chem.*, 2004, **69**, 4433–4440. 2-methylpyridine conjugate has p*K*_a of 5.94. I. Kaljurand, A. Kütt, L. Sooväli, T. Rodima, V. Mäemets, I. Leito and I. A. Koppel, *J. Org. Chem.*, 2005, **70**, 1019–1028.
- 22 A. Gómez-Suárez, D. J. Nelson and S. P. Nolan, *Chem. Commun.*, 2017, **53**, 2650–2660.
- 23 S. N. Sluijter, S. Warsink, M. Lutz and C. J. Elsevier, *Dalton Trans.*, 2013, **42**, 7365–7372.